EXPERIMENTAL INVESTIGATION OF HYDROGEN JET FIRE MITIGATION BY BARRIER WALLS*

R. W. Schefer[1], E. G. Merilo[2], M. A. Groethe[3] and W. G. Houf[4]

[1] Sandia National Laboratories, Livermore, CA 94551-0969, USA, rwsche@sandia.gov
[2] SRI International, Menlo Park, CA 94025-3493, USA, erik.merilo@sri.com
[3] SRI International, Menlo Park, CA 94025-3493, USA, mark.groethe@sri.com
[4] Sandia National Laboratories, Livermore, CA 94551-0969, USA, will@sandia.gov

Abstract

Hydrogen jet flames resulting from ignition of unintended releases can be extensive in length and pose significant radiation and impingement hazards. One possible mitigation strategy to reduce exposure to jet flames is to incorporate barriers around hydrogen storage and delivery equipment. While reducing the extent of unacceptable consequences, the walls may introduce other hazards if not properly configured. This paper describes experiments carried out to characterize the effectiveness of different barrier wall configurations at reducing the hazards created by jet fires. The hazards that are evaluated are the generation of overpressure during ignition, the thermal radiation produced by the jet flame, and the effectiveness of the wall at deflecting the flame.

The tests were conducted against a vertical wall (1-wall configuration), and two "3-wall" configurations that consisted of the same vertical wall with two side walls of the same dimensions angled at 135° and 90°. The hydrogen jet impinged on the center of the central wall. The maximum overpressure measured was 8.31 kPa, which occurred near the release point with the barrier wall in the 3-wall 90° configuration. The highest measured heat fluxes occurred next to the wall's surface. The peak measured heat flux was 19 kW/m^2, which occurred during a test with the 90° side walls. In terms of reducing the radiation heat flux behind the wall, the 1-wall configuration performed best followed by the 3-wall 135° configuration and the 3-wall 90°. The reduced shielding efficiency of the three wall configurations was probably due to the additional confinement created by the side walls that limited the escape of hot gases to the sides of the wall and forced the hot gases to travel over the top of the wall.

The 3-wall barrier with 135° side walls exhibited the best overall performance. Overpressures produced on the release side of the wall were similar to those produced in the 1-wall configuration. The attenuation of overpressure and impulse behind the wall was comparable to that of the three wall configuration with 90° side walls. The 3-wall 135° configuration's ability to shield the back side of the wall from the heat flux emitted from the jet flame was comparable to the 1-wall and better than the 3-wall 90° configuration. The ratio of peak overpressure (from in front of the wall and from behind the wall) showed that the 3-wall 135° configuration and the 3-wall 90° configuration had a similar effectiveness. In terms of the pressure mitigation, the 3-wall configurations performed significantly better than the 1-wall configuration.

1.0 INTRODUCTON

When an accidental high-pressure release of hydrogen is ignited the deflagration that occurs can result in the generation of a significant overpressure. As the jet fire develops, the flame can impinge on objects and emit thermal radiation. One strategy for mitigating these hazards is to use barrier walls to protect people and property in close proximity to the release. Barrier walls can attenuate the effects of overpressure, distort the shape of the flame to prevent it from impinging on sensitive objects, and shield an area from the thermal radiation emitted by a hydrogen jet flame. These walls can also protect an area from fragments that are launched by a failed pressure vessel or an internal explosion that fragments a vessel. However, using a barrier wall can increase the blast overpressure, flame impingement, and the radiation heat flux on the side of the wall that is facing the release. When these

barriers are used to reduce the consequences of a hydrogen jet fire it is important to ensure that they do not create unnecessary additional hazards near the release.

Previous experimental studies related to hydrogen vehicle refueling stations demonstrated that overpressure produced during ignition varied significantly with the ignition time relative to time of release and that both the flow turbulence and the amount of H_2 released effected overpressure (Shirvill et al. [1]; Tanaka et al. [2]). Groethe et al. [3, 4] showed experimentally that barrier walls were effective at reducing overpressure behind the wall and that this reduction extended to at least twice the wall height. Modeling studies reported by Tchouvelev et al. [5] showed that a barrier can reduce the range of the hazardous area by limiting the extent of the flammable gas envelope. Schefer et al. [6-8] reported experimental studies demonstrating that some barrier wall configurations are more effective at mitigating hazards associated with unintended releases.

2.0 EXPERIMENTAL

2.1 Experimental Description and Test Conditions

Three barrier wall configurations were evaluated in this test series. These configurations consisted of a single vertical wall (1-wall), a three sided wall having a single vertical wall and two side walls at a 135^o angle (3-wall 135^o), and a three sided wall with 90^o side walls (3-wall 90^o). Figure 1 shows a schematic and pictures of the three barrier wall configurations. The central vertical wall configuration used in these tests was a 2.4 m wide by 2.4 m tall cinderblock wall. The side walls were constructed out of steel covered with a cement backer board. The hydrogen jet impinged on the center of the cinderblock wall in all tests. Note that the 3-wall 90^o is a new configuration that has not been previously studied. It was selected to characterize the effect of increased confinement on hazards associated with the use of barrier for hazards mitigation.

Details of the hydrogen delivery system can be found in Ref. [9]. The hydrogen was provided by a custom “six-pack” of hydrogen cylinders (13.8 MPa), each individual cylinder with a volume of 43.8 liters, that was modified to remove restrictions in the gas line leading from the cylinder manifold. The hydrogen was delivered to a stagnation chamber located just prior to the jet exit. The stagnation chamber was 26.1 cm in length by 15.3 cm inside diameter and was sized to maintain a low flow Mach number in the stagnation chamber. At this Mach number, the measured pressure and temperature in the stagnation chamber were in excellent agreement with the true stagnation conditions and the jet exit conditions could then be calculated assuming isentropic expansion between the stagnation chamber and the horizontally-orientated, 3.175-mm diameter jet exit. In previous tests a pneumatic valve located between the stagnation chamber and the jet exit prevented flow through the jet nozzle. The pneumatic valve was opened to start a test and allow hydrogen to be discharged through the jet exit. This valve had an opening time of approximately 2-3 seconds and was used only for a repeat of the 3-wall 135^o test from 2007 as a “tie-back”. The long opening time of the pneumatic valve was not desirable for the study of dwell time effects and so it was necessary to use a valve that had a significantly faster response time. To meet this requirement an electrically actuated Tescom VG-C6CBVG9H9 air operated valve was used. This valve has an actuation time of less then 75 milliseconds and was used in all of the remaining tests.

The hydrogen jet was ignited by a spark nominally located 30.5 cm in front of the wall and 12.7 cm off the jet centerline at an angle of 210 degrees from an upward vertical line. Note that in one series of tests the location of the spark location was varied to determine the effect on overpressure produced. A single spark was provided by a spark plug with an approximate energy of 40 Joules. The timing between the spark and the start of the leak could be varied.

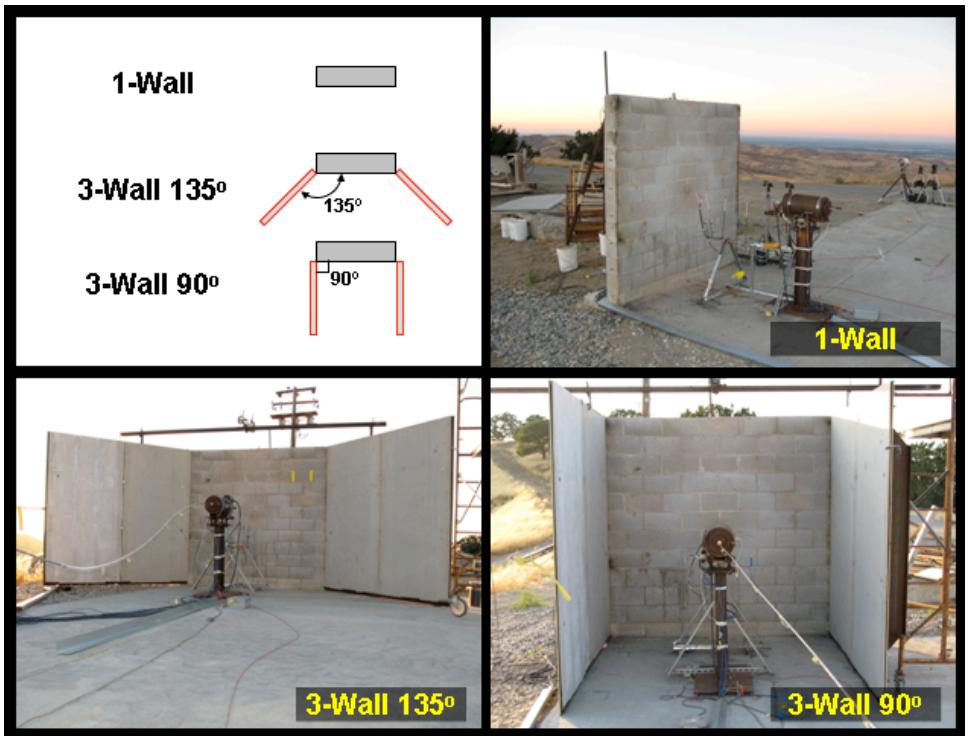

Figure 1. Barrier wall configurations.

2.2 Instrumentation

Standard visible and infrared video camera recordings were used to characterize the flame/wall interactions and the effectiveness of the wall at deflecting the flame. In addition, a high-speed Phantom camera (500-1000 frames per second) provided data on the initial flame ignition process and subsequent propagation.

Other instrumentation included Medtherm Model 64P-1-22 Schmidt-Boelter thermopile detectors (radiometers) to quantify the radiative heat flux from the flame. Two heat flux gauges were located along the flame centerline prior to the wall (typically offset by 1.2 to 1.4 m from the centerline) to determine the radiative heat flux from the undisturbed portion of the free jet flame. In addition, one was located near the jet exit to characterize radiation received at the leak source from the deflected flame, and two were located behind the wall to determine the effectiveness of the wall at mitigating the flame radiation hazard.

Thermocouples were located along the flame centerline leading up to the wall, at various points along the surface of the wall and at a point just behind the wall. The temperature measurements will be used to verify and validate CFD model predictions and to measure heat transfer characteristics. In addition, a displacement sensor was placed on the backside of the wall at the center, approximately 30.5 cm below the top of the wall. This was used to measure the deflection of the wall due to initial impact of the jet flow and the overpressure wave resulting from initial ignition of the hydrogen/air mixture. The wall deflection was measured in Tests 1, 2 and 5 at the same location on the wall.

Piezoelectric pressure transducers were added to the experiments to measure the overpressures that are expected to occur early in the ignition process. Generally, the pressure transducers were placed along

the ground with the sensor face located 6.35 cm above the ground. The transducers located before and after the wall quantify the effectiveness of wall at reducing the effects of overpressures generated during ignition.

This general experimental setup was used for each of the five tests, with some modifications as needed to accommodate the different wall configurations. Voltage outputs from all instrumentation were recorded on Nicolet digital storage scopes for post processing, For each test a weather station was used to record wind speed, wind direction, temperature, humidity and barometric pressure.

Three types of tests were performed in this most recent test series. They were (1) long duration releases in which the hydrogen tank was allowed to blown down to nearly ambient pressure over a period of 300 seconds, (2) dwell tests in which the amount of time between the initiation of the release and the ignition of the jet fire was varied, and (3) spark location tests where the location of the spark was varied along with dwell time.

3.0 RESULTS

3.1 Long Duration Tests

Flame deflection

Standard video was used to determine the effectiveness of the barrier walls at deflecting the flame. Shown in Fig. 2 are single frame images of the three flames studied. The frames were taken at several seconds into the tests after transient effects due to initial hydrogen jet formation and flame ignition have diminished. Shown in Fig. 2a is a single frame for the single wall test. The vertical wall is located along the right side of the frame. The horizontal jet flow exits from the 3.175-mm diameter jet tube, which is located slightly to the left of the image center and the flow direction is left to right. The video image shows a 90 degree upward deflection of the flame, with no apparent flame stabilized behind the wall. The part of the flame that is deflected downward by the wall is seen to turn back toward the jet source as it impacts the ground. Depending on how close the wall is to the hydrogen source (i.e. storage tank, high pressure lines) this flame deflection toward the hydrogen source could result in an additional hazard due to heating of the source and potential equipment failures.

The visible flame image for the three-sided wall with 135 degree angle is shown in Fig. 2b. The video cameras were located higher off the ground and the view of the cameras is over one of the side walls looking downward at an angle to the flame impingement point. The flame is again deflected outward from the wall impact point by the center cinderblock wall. It can be seen that the deflection of the flame does not quite extend outward to the angled side walls. The image for the three-sided wall with 90 degree angle is seen in Fig. 2c. Again the deflected flame does not quite extend to the side walls.

High-speed video was used to capture the development of the flame in the period just after ignition, when the flame front propagates out from the spark location to its maximum size. Shown in Fig.3 are selected individual high-speed video frames from the single-wall configuration. In contrast to previous tests [6], two high speed video cameras were used simultaneously at frame rates up to 7,000 frames per second to detect the flame development from multiple angles. The three frames in the top row of the figure were taken from a camera located behind the leak exit and looking perpendicular to the barrier wall while the frames in the bottom row were taken with the camera located to the side of the developing flame. The framing rates are also significantly higher than the 500 fps frame rates used in previous tests to show more details of the flame development. The frames shown in these figures are representative frames that show the initiation of the jet flame and the first 70 milliseconds of flame

expansion during each of the three tests. The high-speed video shows that at the time that the pressure waveforms have been detected by the closest pressure transducer, approximately 4 milliseconds to 10 milliseconds after initiation, only a portion of the flammable gas mixture has combusted. Similar results are seen with both the 3-wall 135° test, and the 3-wall 90° test configurations.

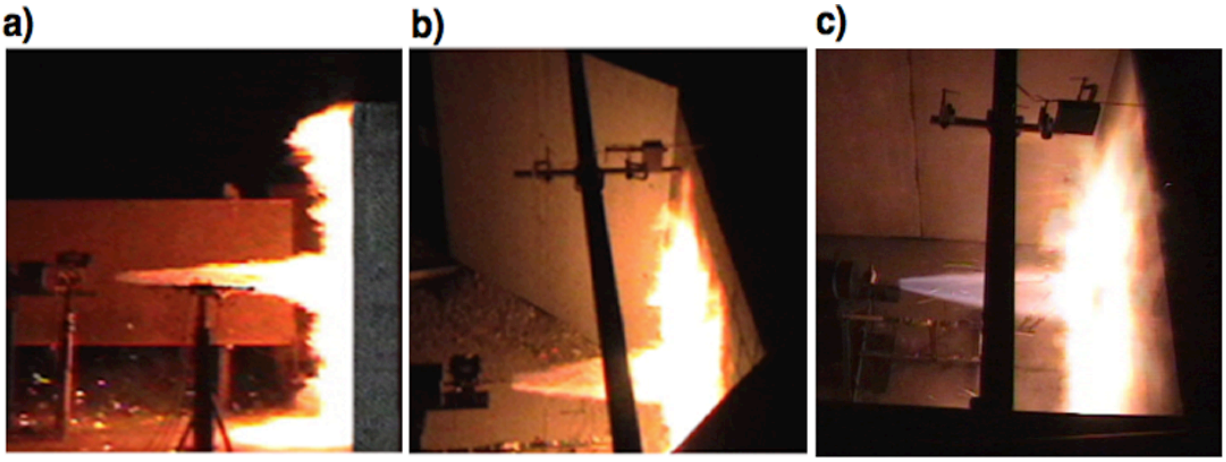

Figure 2. Standard video frames from 3-wall configurations. (a) 1-Wall; (b) 3-Wall 135; (c) 2-Wall 90°

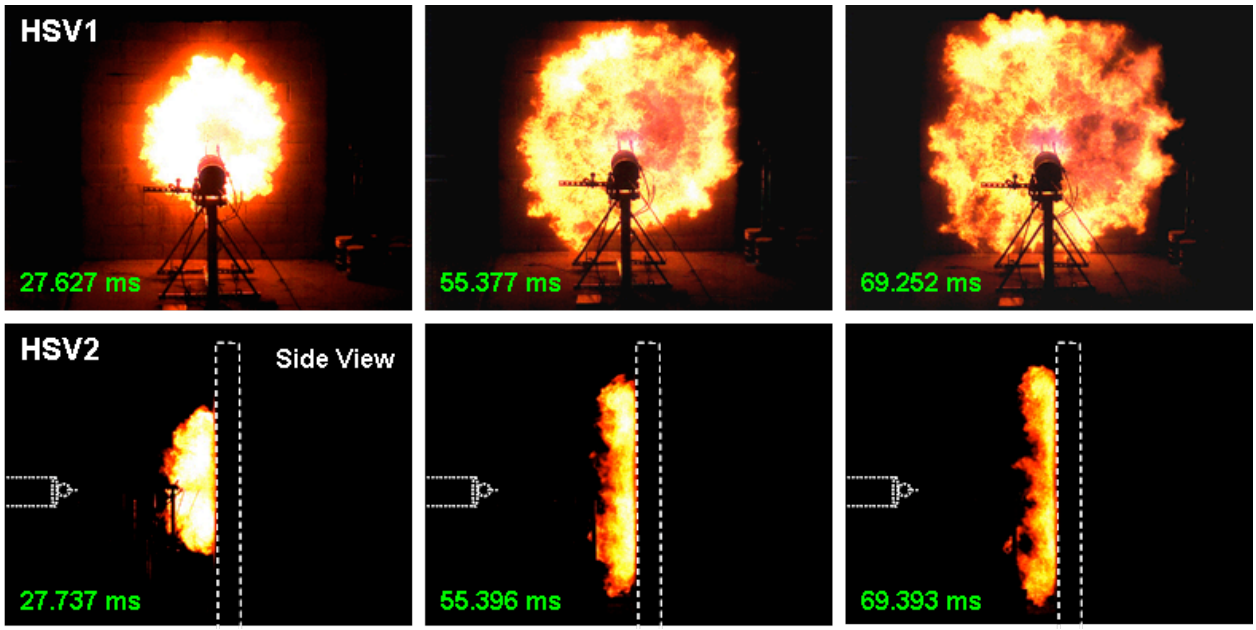

Figure 3. High-speed video frames from 1-wall configuration, Test 33-08.

Overpressure measurements

Pressure transducers mounted on the ground were used to measure the overpressure and impulse on both sides of the barrier walls. These measurements allow the effectiveness of different wall configurations to be evaluated. Figure 4 shows a comparison of representative pressure and impulse

waveforms measured in front of and behind the barrier wall in each of the three barrier wall configurations. These waveforms are representative of the typical waveforms seen throughout the test series and are reasonable for making a comparison. The plot for the release side of the barrier, Fig. 4a, shows that the 1-wall and the 3-wall 135° configurations produce similar waveforms, while the waveform in the 3-wall 90° configuration has multiple peaks. This second peak is produced when pressure wave reflects off of the barrier's side walls. These reflections lead to significantly higher peak pressures and greater impulse. Both of these factors can lead to an increased potential for damage to structures near the leak source.

The plot comparing the waveforms in the reduced pressure region behind the barrier wall, Fig. 4b, shows that the 3-wall 90° and the 3-wall 135° had similar performance. In the 1-wall configuration the overpressure and impulse measured behind the barrier were significantly higher than both of the 3-wall configurations. Based on the overpressure measured near the source and behind the barrier these results indicate that the 3-wall 135° is the best wall for protecting an area from overpressure without significantly increasing the hazards near the release point. It matches the performance of the best features for the other two wall configurations.

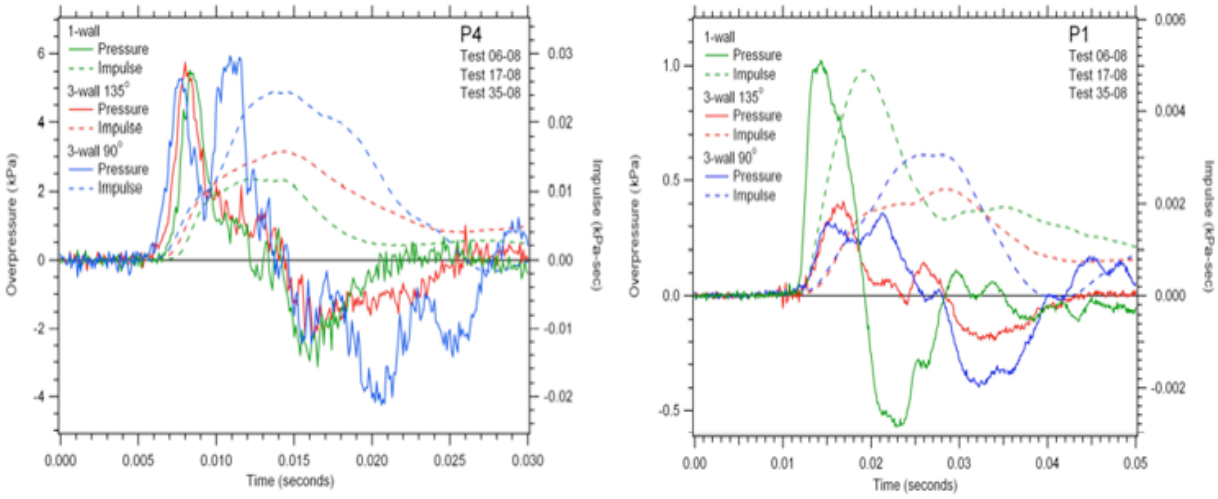

Figure 4. Comparison of pressure and impulse waveforms for the 1-wall, 3-wall 135°, and 3-wall 90° configurations. (a) Measured in front of wall; (b) Measured behind wall.

Flame radiation

The heat flux emitted by the hydrogen jet flame was measured with radiometers in front of and behind the barrier wall. Figure 5a shows a comparison of heat flux measured by radiometer R1 for the three different wall configurations. R1 was positioned near the release point and had of view of the approximately half of the cinderblock wall's surface and when present, one of the barrier's side walls. The heat flux imparted to an object located at the release point with the unobstructed view of the entire surface of the wall would experience a heat flux of roughly twice what was measured by R1. This plot shows that the 3-wall 90° configurations produced the highest heat fluxes near the release point followed by the 3-wall 135° configuration with the single-wall configuration producing the lowest heat flux.

Figure 5b shows the comparisons of the measurements by radiometer R6 made behind the barrier wall for the three different wall configurations. Radiometer R6 was located at the height of the wall, looking directly at the wall's top edge and 1.41 m behind the wall. The results show that the 3-wall 90°

configuration emitted the highest level of thermal radiation behind the wall. The higher heat flux seen in the 3-wall 90° configuration are probably caused by the configurations greater confinement. The air trapped in the middle of the 3-wall 90° configuration can not be cooled as efficiently as it can in the other configurations. The side walls force most of the hot gases to be vented above the wall while the other configurations may allow some of the hot gases to escape towards the sides. The confinement may cause the flame to expand higher above the edge of the wall in the 3-wall 90° configuration thereby increasing the thermal radiation seen behind the barrier. This phenomena will depend on the size of the jet fire. If a larger release was studied with the same barrier wall configurations there may be more significant differences between the three different wall configurations ability to protect the area behind the wall from thermal radiation. If the same release impinged on a larger barrier wall there may be little difference between the three configurations.

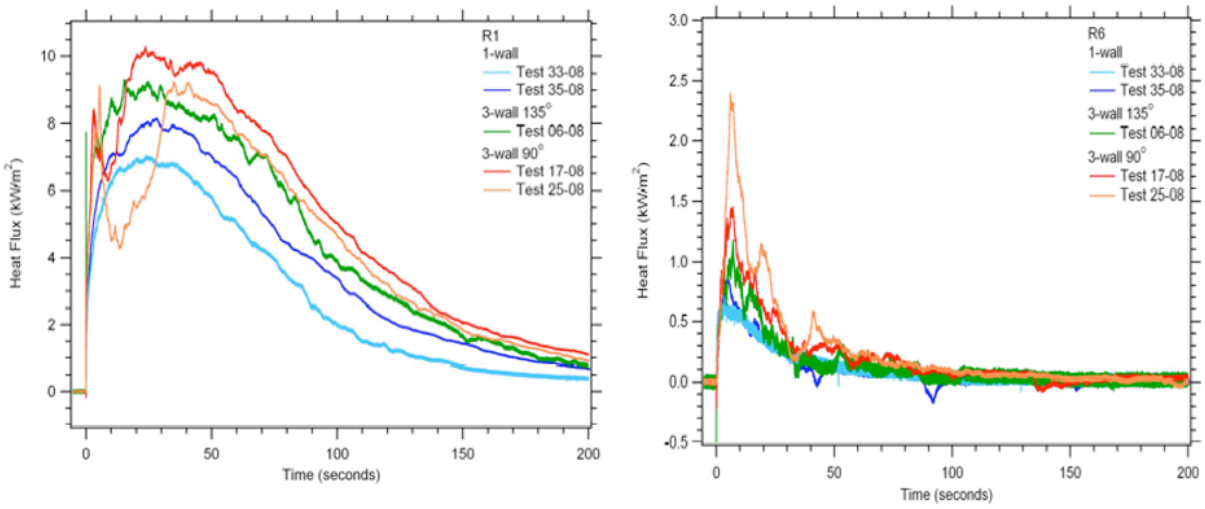

Figure 5. Comparson of radiative heat flux measured in the 1-wall, 3-wall 135°, and 3-wall 90° configurations. (a) In front of wall (R1); (b) Behind wall (R6).

3.2 Dwell Tests

Experiments were completed to characterize the effect of ignition delay time, ignition location and barrier wall configuration on the overpressure produced during the ignition of hydrogen leaks. The ignition delay is defined as the time between the start of the hydrogen leak and the firing of the ignition spark. The ignition location was varied by moving the spark ignitor to different locations in the flow. For the ignition delay time tests the spark ignitor location was kept at the same location as in previous barrier wall tests where the spark was located 30.5 cm in front of the wall and 12.7 cm off the jet centerline at an angle of 210 degrees from an upward vertical line. This location corresponds to the estimated position of the mixing layer adjacent to the hydrogen jet where the hydrogen has mixed with sufficient air to form a flammable mixture and the velocity is low enough to allow flame propagation upstream where a stable flame is formed. Previous model calculations carried out using the FLACS code [10] indicate that the overpressure rises rapidly for ignition delay times during the first 500 msec to 1 sec after the hydrogen release is initiated and then levels off to a nearly constant value for ignition delay times greater than this. Shown in Fig. 6a are the peak measured overpressures in front of the wall as a function of ignition delay time. The delay time was varied from a minimum of 40 msec to a maximum of about 6 seconds after leak initiation. Results are shown for the single vertical wall and the three-sided walls with angles of 135 degrees and 90 degrees. The single wall showed the lowest peak overpressure 5.44 kPa (0.79 psi). Somewhat higher pressures of 5.86 kPa (0.85 psi) and 7.17 kPa (1.04 psi) were measured for the three-sided walls with 135 degree and 90 degree angles, respectively.

As might be expected, the overpressure increases due to the increased confinement as side walls are added and the angle between the walls is reduced. It is also seen that with all three-wall configurations the overpressure remains nearly constant over the range of delay times studied. While this general behavior agrees with the FLACS model calculations, the experiments did not show the predicted decrease in the overpressure at the shortest delay times measured. This behavior implies that the mixing between hydrogen and ambient air that leads to a combustible mixture occurs quite rapidly. The corresponding overpressure impulse, which is the integral over time of the pressure pulse, is shown in Fig. 6b. Structures respond to both overpressure magnitude and impulse. Thus, high overpressure for a short duration or low overpressure for a long duration can cause significant structural damage. The impulse produced by the three-sided, 90 degree wall is nearly a factor of 2 larger that either the 135 degree wall angle or the single wall.

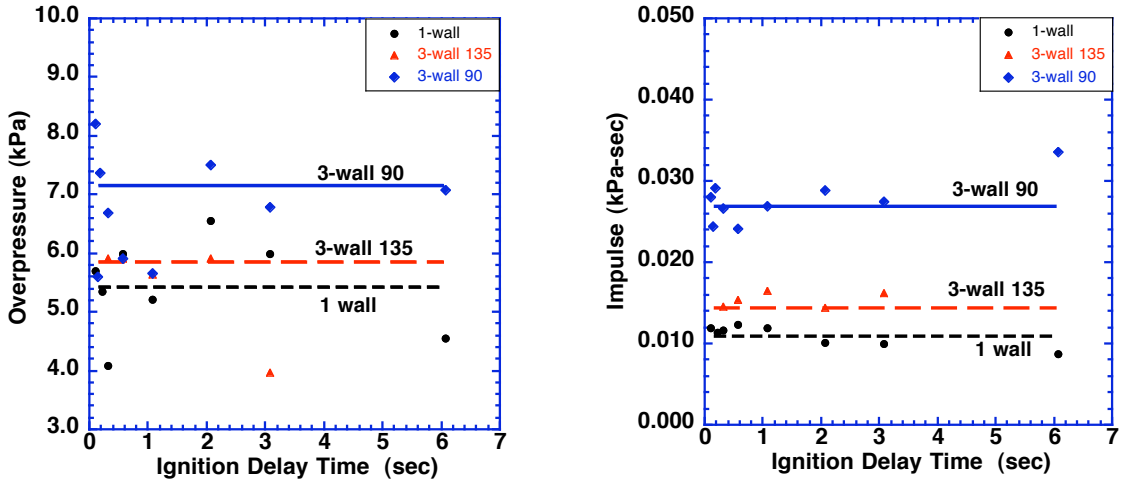

Figure 6. The variation in overpressure with delay time for single wall, three-sided wall with 135 degree angle, and three-sided wall with 90 degree angle. Pressure transducer located in front of wall. (a) Overpressure; (b) Impulse.

Figure 7 shows a comparison of the overpressure measured in front of the wall and behind the wall for each of the configurations. All three configurations are effective at reducing the overpressure hazard. For example, the single wall reduces the overpressure behind the wall by about a factor of 5, while the three-sided walls reduce the overpressure by nearly a factor of 20.

3.3 Ignition Location Tests

As noted above, moving the spark igniter to different positions in the flow allows the ignition location to be varied. Shown in Fig. 8 are the overpressures measured in the three-sided 90 degree wall configuration for three spark igniter locations. The locations 1 through 3 are indicated in the insert to Fig. 8 as Spark 1, 2 and 3 New. No flame could be ignited with the spark located at the fourth position, Spark 3, probably due to the presence of a nonflammable hydrogen/air mixture there. Within the variability of the overpressure measurement (indicated by the error bars) the overpressure produced is insensitive to ignition location. This observation is in agreement with FLACS calculations.

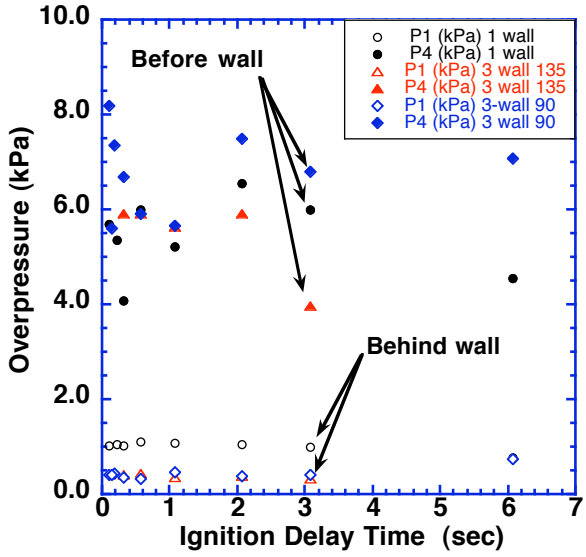

Figure 7. The effect of delay time on overpressure produced in front of wall (solid symbols) and behind wall (open symbols) for single wall, three-sided wall with 135 degree angle, and three-sided wall with 90 degree angle.

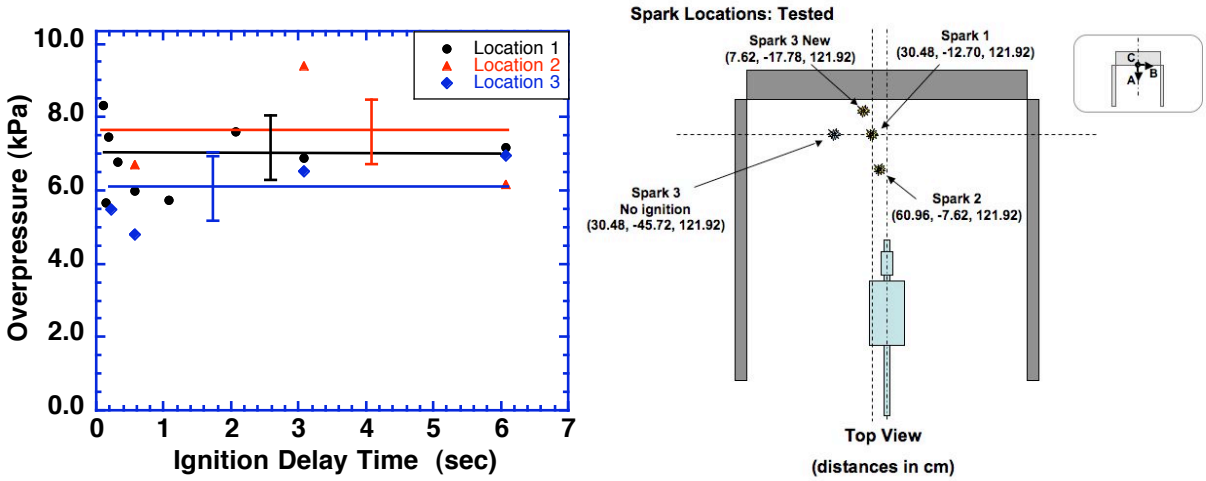

Figure 8. The effect of ignition location on overpressure produced in front of three-sided wall with 90 degree angle.

4.0 CONCLUSIONS

The results of this study show that the 3-wall 135° configuration was the most effective overall at mitigating the effects of overpressure and thermal radiation caused by the ignition of a hydrogen jet. The overpressures, measured near the release point, on the protected side of the wall, were the same as those produced in the 1-wall configuration and the impulse was only a small amount higher. The 3-wall 135° configuration attenuated overpressure as well at the three wall configuration with 90° side walls and the impulse on the protected side of the wall was the lowest of the three barrier configurations. The heat flux measured near the release point was lower than the 3-wall 90° configuration, but not as low as the 1-wall configuration. The thermal radiation that the flame emitted

to the back side of the wall was only slightly higher then the 1-wall configuration.

These results illustrate the differences in mitigating performance of the different barrier wall designs. It has been shown that in the 3-wall 90° configuration, the pressure waves that reflect off the side walls play a significant role in increasing the hazard near the leak source. These reflected waves can significantly increase the peak overpressure in certain locations as well as increasing the impulse. Both of these factors will lead to an increased probability of damage to structures near the leak source. The dwell time tests, where the ignition time was varied from 0.04 sec to 6.00 sec after the start of the release, showed relatively constant peak overpressure and impulse for all three wall configurations. This result indicates that there was enough flammable gas present to produce the observed overpressure and impulse within 70 milliseconds after the valve started to open.

Tests performed to evaluate how the ignition location affected the overpressure and impulse were conducted with the 3-wall 90° configuration. The results showed that in this configuration the spark location was not important. However, the waveform structure was dependent on the spark location due to variations in the transit path of the incident pressure wave and the waves reflected from the wall surface.

Comparing the ratio of peak overpressure and impulse measured in front of a wall to that measured in back of the wall showed that for the 3-wall 90° configuration there was a decrease in the walls effectiveness as the ignition time was delayed. This result is not a safety concern because the magnitude of the change in overpressure and impulse behind the barrier wall was relatively small. The other two wall configurations did not show a clear trend.

5.0 ACKNOWLEDGMENTS

This research was supported by the United States Department of Energy, Office of Energy Efficiency and Renewable Energy, Hydrogen, Fuel Cells and Infrastructure Technologies Program. Sandia is operated by the Sandia Corporation, a Lockeed Martin Company, for the U.S. DOE under contract No. DE-AC04-94-AL8500. This work was monitored by Antonio Ruiz under contract No. DE-AC04-94-AL8500.

6.0 REFERENCES

1. Shirvill, L.C. and Roberts, T.A., “Designing for Safe Operations: Understanding the Hazards Posed by High Pressure Leaks from Hydrogen Refuelling Stations,” 2006 NHA Conference, March 12-16, Long Beach, CA, 2006.
2. Tanaka, T., Azuma, T., Evans, J.A., Cronon, P.M., Johnson, D.M. and Cleaver, R.P., “Experimental Study on Hydrogen Explosions in a Full-Scale Hydrogen Filling Station,” HYSAFE ICHS International Conference on Hydrogen Safety, Paper 120036, Pisa, Italy, Sept. 8-10, 2005.
3. Groethe, M., Colton, J., Chiba, S. and Sato, Y., “Hydrogen Deflagrations at Large Scale,” 15th World Hydrogen Energy Conference, June 27-July 2, 2004, Yokohama, Japan.
4. Groethe, M., Merilo, E., Colton, J., Chiba, S., Sato, Y. and Iwabuchi, H., “Large-scale Hydrogen Deflagrations and Detonations,” Int. J. of Hydrogen Energy, 32, 13, 2125-2133, 2007.
5. Tchouvelev, A.V., Cheng, Z, Agranat, V.M. and Zhubrin, S.V., “Effectiveness of Small Barriers as Means to Reduce Clearance Distances,” Int. Jour. of Hydrogen Energy, Vol. 32, 1409-1415, 2007.
6. Schefer, R.W., Groethe, M., Houf, W.G., Evans, G.H., “Experimental Evaluation of Barrier Walls for Risk Reduction of Unintended Hydrogen Releases,” Int. Jour. of Hydrogen Energy, Vol. 34, 1590-1606, Feb. 2009.
7. Schefer, R.W., Houf, W.G., Groethe, M., Evans, G., Royle, M., Willoughby, D., “HYPER Report 5.4 – Report on Experimental Evaluation of Barrier Walls for Risk Reduction of Unintended

Releases of Hydrogen," Sept. 30, 2008.
8. Schefer, R.W., Groethe, M., Houf, W.G. and Evans, G., "Experimental Evaluation of Barrier Walls for Risk Reduction of Unintended Hydrogen Releases," Sandia Report SAND2008-41411, October, 2008.
9. Schefer, R.W., Houf, W.G., Williams, T.C. Bourne, B., and Colton, J., "Characterization of High-Pressure, Underexpanded Hydrogen-Jet Flames," Int. J. of Hydrogen Energy, **32**, 12, 1132-1140, 2007.
10. FLACS Version 8 Users Guide, GEXCON, Bergen, Norway, 2003.